Phase transformation in nanocrystalline α-quartz GeO_2 up to 51.5 GPa

2006 J. Phys.: Condens. Matter 18 10817

(http://iopscience.iop.org/0953-8984/18/48/008)

INSTITUTE OF PHYSICS PUBLISHING JOURNAL OF PHYSICS: CONDENSED MATTER

J. Phys.: Condens. Matter **18** (2006) 10817–10824 doi:10.1088/0953-8984/18/48/008

Phase transformation in nanocrystalline α-quartz GeO_2 up to 51.5 GPa

H Wang[1], J F Liu[1], H P Wu[1], Y He[1], W Chen[1], Y Wang[1], Y W Zeng[1,2], Y W Wang[1,2], C J Luo[3], J Liu[3], T D Hu[3], K Stahl[4] and J Z Jiang[1,5]

[1] Laboratory of New-Structured Materials, Department of Materials Science and Engineering, Zhejiang University, Hangzhou 310027, People's Republic of China
[2] Center for Analysis, Zhejiang University, Hangzhou 310027, People's Republic of China
[3] Institute of High Energy Physics, Chinese Academy of Sciences, Beijing, People's Republic of China
[4] Department of Chemistry, Technical University of Denmark, DK-2800 Lyngby, Denmark

E-mail: jiangjz@zju.edu.cn

Received 18 April 2006, in final form 23 August 2006
Published 17 November 2006
Online at stacks.iop.org/JPhysCM/18/10817

Abstract

The high-pressure behaviour of nanocrystalline α-quartz GeO_2 (q-GeO_2) with average crystallite sizes of 40 and 260 nm has been studied by *in situ* high-pressure synchrotron radiation x-ray diffraction measurements up to about 51.5 GPa at ambient temperature. Two phase transformations, q-GeO_2 to amorphous GeO_2 and amorphous GeO_2 to monoclinic GeO_2, are detected. The onset and end of the transition pressures for the q-GeO_2-to-amorphous GeO_2 phase transition are found to be approximately 10.8 and 14.9 GPa for the 40 nm q-GeO_2 sample, and 9.5 and 12.4 GPa for the 260 nm q-GeO_2 sample, respectively. The mixture of amorphous and monoclinic GeO_2 phases remains up to 51.5 GPa during compression and even after pressure release. This result strongly suggests that the difference of free energy between the amorphous phase and the monoclinic phase might be small. Consequently, defects in the starting material, which alter the free energies of the amorphous phase and the monoclinic phase, may play a key role for the phase transformation of q-GeO_2.

Germanium oxide (GeO_2) at ambient pressure has two polymorphs: α-quartz and rutile-type structures with fourfold- and sixfold-coordinated germanium ions, respectively. The rutile structure of GeO_2 is stable under ambient conditions [1]. The great interest in α-quartz GeO_2 (q-GeO_2) comes from the similarity to the α-quartz SiO_2, which possesses wide implications in geophysics. A phase transition of q-GeO_2 above 6 GPa has been observed with various techniques: x-ray diffraction (XRD), x-ray absorption fine structure (XAFS), and Raman spectroscopy [2–14]. However, there are discrepancies between the results reported from

[5] Author to whom any correspondence should be addressed.

different groups. A high-pressure amorphous phase of polycrystalline q-GeO_2 above 6 GPa has been reported [2–4]. Many explanations from different views were proposed to understand the crystalline-to-amorphous transition. A thermodynamic melting mode was proposed in metastable quartz, which was reported to become amorphous above 30 GPa [15, 16]. Wolf *et al* [17, 18] found that the free energy of the germania glass at room temperature is equal to that of the metastable crystalline quartz phase at a pressure of 7.5 ± 1 GPa. An instability in the tetrahedral network at high pressure leads to a change in the cation coordination number and the precipitation of the crystalline-to-amorphous transition. Meanwhile, a high-pressure phase with monoclinic structure ($P21/c$) was also observed [11–14]. The transition in single-crystalline q-GeO_2 was suggested to be a coherent cooperative atomic motion. For polycrystalline q-GeO_2, the coherent displacive transition is hindered from the dispersion of stresses in individual crystallites and a large portion of defective atomic sites at grain boundaries [11]. It is known that nanometre-sized crystals, due to the high density of grain boundaries, often have novel physical and chemical properties, differing from those of the corresponding bulk materials [19]. For example, the transition pressure for crystal-to-crystal phase transformation strongly depends on crystallite size in the nanometre region [20]. Furthermore, in most cases, q-GeO_2 samples with larger crystallite sizes were used to study the phase transition above 6 GPa. In this work, we report an *in situ* high-pressure synchrotron radiation x-ray diffraction study of q-GeO_2 nanocrystals with average crystallite sizes of 40 nm up to 51.5 GPa and an average crystallite size of 260 nm up to 40.6 GPa at ambient temperature.

Nanometre-sized q-GeO_2 crystallites with average sizes of 40 and 260 nm were prepared by the reverse micelle technique. Germanium chloride ($GeCl_4$), heptane, and water were used as precursor, oil phase, and water phase, respectively. Oleylamine and cetyltrimethylammonium (CTAB) were used as surfactant. Details for sample preparation can be found in [21]. The average crystallite size and size distribution of q-GeO_2 nanoparticle samples were determined by x-ray diffraction (X'TRA-XRD) using a Cu Kα radiation and high-resolution transmission electron microscopy (HRTEM) (JEM-2010). Figure 1 shows the XRD pattern, TEM image and grain size distribution for one of the q-GeO_2 nanocrystalline samples studied. It is found that all of the reflection peaks in the XRD pattern can be indexed to a pure hexagonal phase (space group: ($P21/c$)) of q-GeO_2 with a lattice constant of $a = 4.993$ Å and $c = 5.661$ Å, to be consistent with the reported values of $a = 4.987$ Å and $c = 5.652$ Å (PCPDF no. 04-0498). The nanocrystalline q-GeO_2 sample has an average grain size of 40 nm from TEM measurements and 39.1 nm estimated from XRD line broadening. The second sample was also found to be the hexagonal q-GeO_2 phase with a size distribution of 250–270 nm and an average grain size of 260 nm. *In situ* high-pressure energy-dispersive XRD measurements up to about 51.5 GPa were performed at Beijing Synchrotron Radiation Facility at ambient temperature for two nanocrystalline q-GeO_2 samples. The powders were mounted in a 300 μm diameter hole of the T301 stainless steel gasket in a Mao–Bell diamond-anvil cell. A pressure transmitting medium of 4:1 methanol:ethanol solution was used. The actual pressure was measured by the ruby fluorescence method, using the nonlinear pressure scale of Mao *et al* [22].

Figure 2 shows the XRD patterns for 40 nm q-GeO_2 nanocrystals recorded at different pressures during compression up to 51.5 GPa. It is clear that broad amorphous-like XRD patterns were observed at pressures above 10.8 GPa. Figure 3 shows the d value and full width at half maximum (FWHM) of the diffraction peak (101) (located at about 14 keV) as a function of pressure in the range 0–10.8 GPa. It should be noted that due to the overlapping of peaks, only the (101) peak can be used for data analyses. It is found that below 10.8 GPa, the FWHM remains almost constant, indicating that the grain size did not change during compression up to 9.4 GPa. If the broad amorphous-like XRD patterns recorded at above 10.8 GPa were

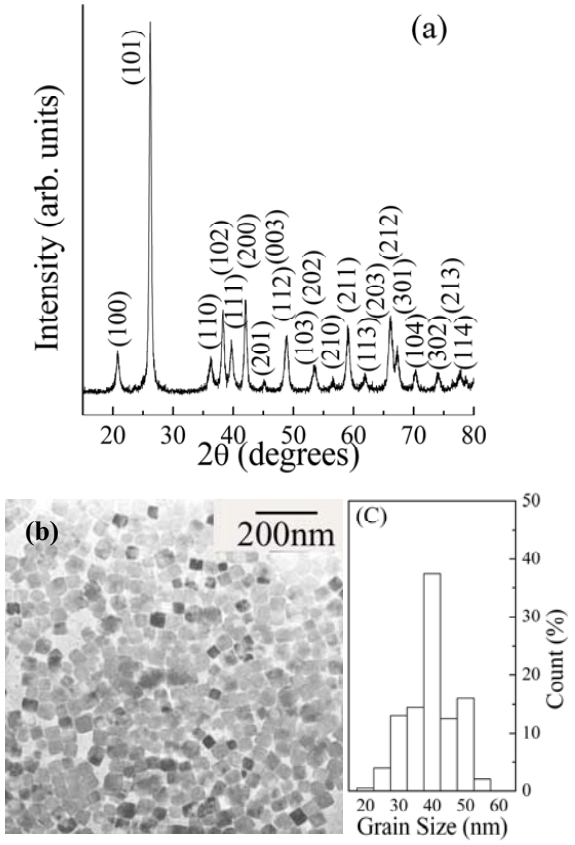

Figure 1. XRD pattern (a), TEM image (b) and grain size distribution (c) for one of the nanometre-sized q-GeO_2 crystallite samples studied here.

composed of small nanometre-sized q-GeO_2 nanocrystals (e.g., <2 nm), then the grain size of q-GeO_2 nanocrystals should be reduced from 40 nm to a few nm during compression. This was not observed in the present work, as shown in figure 3. The onset pressure for the q-GeO_2-to-amorphous GeO_2 transition is approximately 10.8 GPa while the end of the transition is at approximately 14.9 GPa. On further increasing the pressure (see figure 2(b)), the broad amorphous-like XRD patterns remain until 22.8 GPa. At 26.9 GPa, some broad diffraction maxima, marked by arrows, p1, p2, and p3, are superimposed on the broad amorphous-like pattern. We roughly estimated the peak positions for p1, p2, and p3 and found that they could be matched to peaks $(21\bar{1})$, $(20\bar{2})$, and (300) of the monoclinic structure ($P21/c$) phase, respectively. Such a feature remains up to 51.5 GPa. It seems that the disordered amorphous GeO_2 phase formed above 10.8 GPa might recrystallize into the monoclinic structure ($P21/c$) phase with very small grain sizes during further compression. It should be mentioned that the onset pressure for the amorphous-to-monoclinic phase transition is impossible to be estimated due to the poorly crystalline monoclinic phase. But, the monoclinic structure ($P21/c$) phase should be formed at 26.9 GPa. A similar phenomenon was also reported in α-quartz SiO_2 compressed under nonhydrostatic condition [23] and in berlinite-type $FePO_4$ [24]. Figure 4 shows XRD patterns recorded during decompression for 40 nm q-GeO_2 nanocrystals after compression up to 51.5 GPa. The XRD patterns do not change much during decompression. The sample after pressure release consists of a mixture of amorphous and monoclinic structure phases.

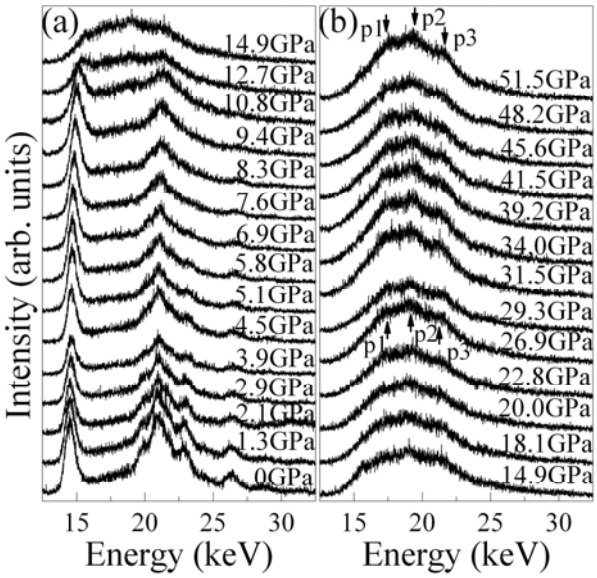

Figure 2. *In situ* high-pressure energy-dispersive synchrotron radiation XRD patterns for nanocrystalline q-GeO_2 with an average crystallite size of 40 nm recorded during compression up to about 51.5 GPa at ambient temperature. Energy (E) times d spacing (d): $Ed = 0.619927/\sin = 48.999\,47$ keV Å. p1, p2, and p3 in figure 2(b) are marked for three peaks $(21\bar{1})$, $(20\bar{2})$, and (300) of the monoclinic phase, respectively.

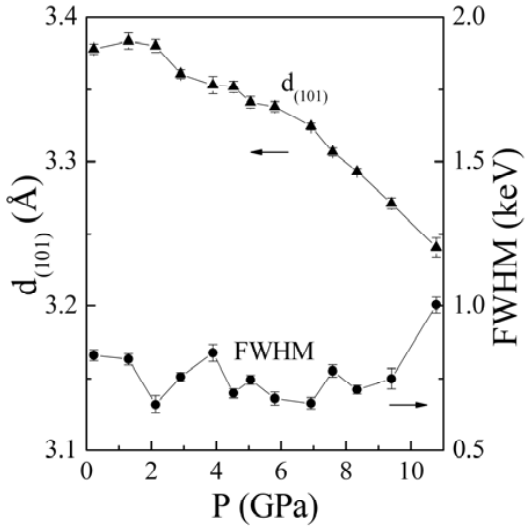

Figure 3. d value and FWHM of the peak (101) for the q-GeO_2 phase as a function of pressure up to 10.8 GPa for nanocrystalline q-GeO_2 with an average crystallite size of 40 nm recorded during compression.

To further confirm the formation of the amorphous-like GeO_2 phase during compression, a second nanocrystalline q-GeO_2 sample with an average grain size of 260 nm under the same compression conditions was studied, as shown in figure 5. The data quality is better than in figure 2 due to long exposure time and large grain size. It is clear that the intensity of the (101) peak of the q-GeO_2 phase is dramatically reduced at a pressure of 9.5 GPa in figure 5(a). The pattern recorded at 12.4 GPa in figure 5(b) is a characteristic one for an amorphous-like

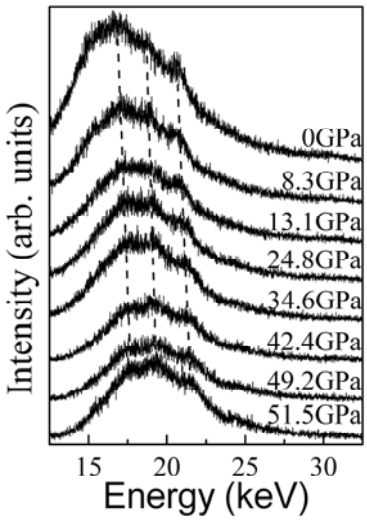

Figure 4. *In situ* high-pressure energy-dispersive synchrotron radiation XRD patterns recorded during decompression for 40 nm q-GeO_2 nanocrystals after compression up to 51.5 GPa. The dashed lines for p1, p2, and p3 peaks are guides for the eyes.

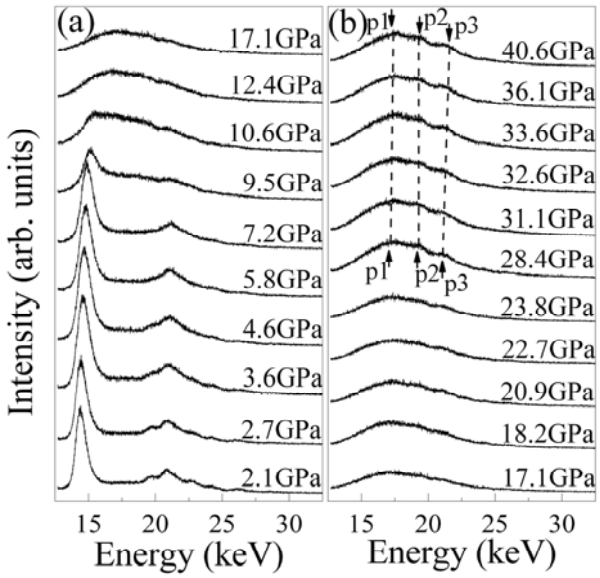

Figure 5. *In situ* high-pressure energy-dispersive synchrotron radiation XRD patterns for nanocrystalline q-GeO_2 with an average crystallite size of 260 nm recorded during compression up to about 40.6 GPa at ambient temperature. Energy (E) times d spacing (d): $Ed = 0.619927/\sin = 48.999\,47$ keV Å. p1, p2, and p3 in (b) are marked for three peaks $(21\bar{1})$, $(20\bar{2})$, and (300) of the monoclinic phase, respectively.

phase. The onset pressure for the q-GeO_2-to-amorphous GeO_2 transition is approximately 9.5 GPa, while the end of the transition is at approximately 12.4 GPa. The amorphous-like x-ray patterns observed here should come from our GeO_2 powder sample because Ge fluorescence

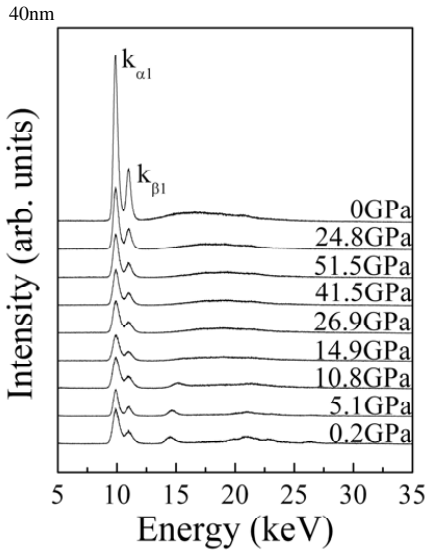

Figure 6. Existence of Ge fluorescence peaks (Kα and Kβ) in some selected *in situ* high-pressure energy-dispersive synchrotron radiation XRD patterns recorded for 40 nm q-GeO_2 nanocrystals after compression and decompression.

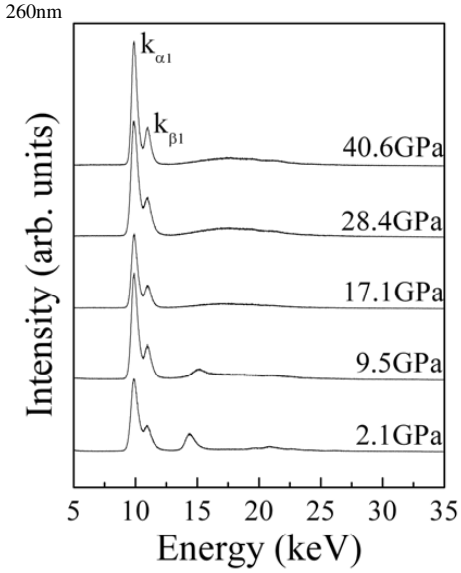

Figure 7. Existence of Ge fluorescence peaks (Kα and Kβ) in some selected *in situ* high-pressure energy-dispersive synchrotron radiation XRD patterns recorded for 260 nm q-GeO_2 nanocrystals after compression.

lines are detected in all XRD patterns recorded here, as shown in figures 6 and 7. On further compression, the broad amorphous-like pattern remains. At 20.9 GPa, three broad peaks for the monoclinic phase, marked by p1, p2, and p3 in figure 5(b), appear, which are similar to those for the 40 nm nanocrystalline sample in figure 2(b). To monitor the change of XRD pattern for the monoclinic phase, we further performed a simulation for the phase with various grain sizes, as shown in figure 8. It is seen that even for 2 nm grain size, the broad diffraction peaks for the phase can still be detected, which is consistent with XRD patterns recorded at above 28.4 GPa for the 260 nm sample in figure 5(b) and at above 22.8 GPa for the 40 nm sample in figure 2(b). The simulated XRD patterns for the monoclinic phase with grain sizes larger than 1 nm are very different from the amorphous-like patterns recorded for both 40 and

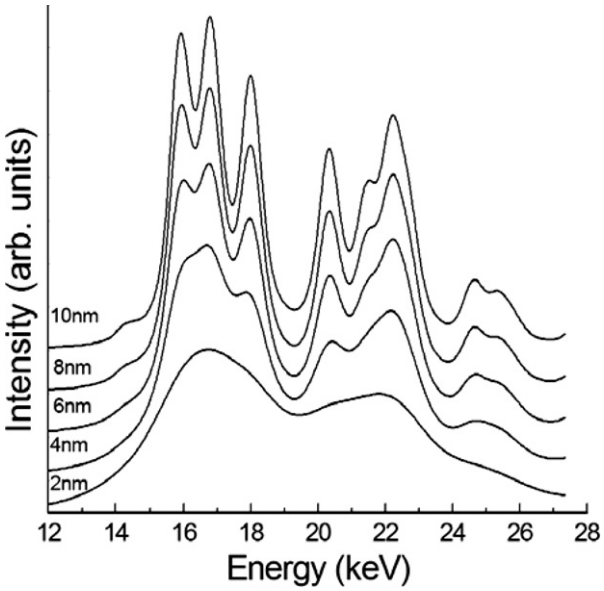

Figure 8. Simulated XRD patterns for the monoclinic phase with various grain sizes.

260 nm nanocrystalline samples in figures 2 and 5. Therefore, two phase transformations, i.e., q-GeO_2 to amorphous GeO_2 and amorphous GeO_2 to monoclinic GeO_2, are indeed detected in the nanocrystalline q-GeO_2 samples studied here.

Two phase-transformation routes for q-GeO_2 have been reported in the literature. They are (1) the q-GeO_2-to-amorphous GeO_2 transition and (2) the q-GeO_2-to-monoclinic GeO_2 transition. The monoclinic phase arises from a coherent cooperative atomic motion [11]. Amorphous transformation is similar to a melting process. The mixture of amorphous and monoclinic GeO_2 phases remains up to 51.5 GPa during compression and even after pressure release. This experimental observation strongly suggests that the difference of free energy between the amorphous phase and the monoclinic phase might be small. Consequently, defects in the starting material, which balance the competition between the amorphous phase and the monoclinic phase, may play a key role for the phase transformation of q-GeO_2. When the average grain size is large, the number of defects, e.g., grain boundaries, is small. The tendency to form the amorphous phase during the compression of q-GeO_2 could be restrained. The high-pressure phase tends to be the crystalline monoclinic phase, as observed for single-crystalline q-GeO_2 [11]. When the average grain size is smaller, the defect density is higher and the amorphous phase might be favoured from the free energy point of view, which is consistent with the results reported here and in [2–4]. On further compression, recrystallization of the amorphous phase could be induced. Consequently, the amorphous GeO_2-to-monoclinic GeO_2 transition occurs, as detected in the present work. More studies are still required to uncover the origin of the two phase-transformation routes for q-GeO_2.

In conclusion, high-pressure behaviours of nanocrystalline q-GeO_2 with average crystallite sizes of 40 and 260 nm have been studied by *in situ* high-pressure synchrotron radiation x-ray diffraction measurements up to about 51.5 GPa at ambient temperature. Two phase transformations, q-GeO_2 to amorphous GeO_2 and amorphous GeO_2 to monoclinic GeO_2, are detected. The onset and end of the transition pressure for the q-GeO_2-to-amorphous GeO_2 phase transition are found to be approximately 10.8 and 14.9 GPa for the 40 nm q-GeO_2 sample, and 9.5 and 12.4 GPa for the 260 nm q-GeO_2 sample, respectively. Based on the experimental observations of coexistence of amorphous and monoclinic GeO_2 phases in the sample up to

51.5 GPa during compression and even after pressure release, we suggest that the free energy of the amorphous phase could be similar to that of the monoclinic phase. Consequently, defects in the starting material, which balance the competition between the amorphous phase and the monoclinic phase, may play a key role for the phase transformation of q-GeO_2, which might cause the discrepancy for the phase transformation of q-GeO_2 above 6 GPa reported in the literature. This work might trigger more studies to uncover the nature of the grain-size effect on phase-transformation routes for q-GeO_2.

Acknowledgments

The authors would like to thank BSRF in Beijing, and NSRL in Hefei, PR China; HASYLAB in Hamburg, Germany; MAX-Lab in Lund, Sweden; and KEK and SPring8 in Japan for the use of the synchrotron radiation facilities. Financial support from the National Natural Science Foundation of China (Grant Nos 50341032 and 50425102), the Ministry of Science and Technology of China (Grant Nos 2004/249/37-14 and 2004/250/31-01A), the Ministry of Education of China (Grant Nos 2.005E+10 and 2005-55) and Zhejiang University is gratefully acknowledged.

References

[1] Hill V G and Chang L L Y 1968 *Am. Mineral.* **53** 1744
[2] Kawasaki S, Ohtaka O and Yamanaka T 1994 *Phys. Chem. Minerals* **20** 531
[3] Kawasaki S 1996 *J. Mater. Sci. Lett.* **15** 1860
[4] Yamanaka T, Nagai T and Tsuchiya T 1997 *Z. Kristallogr.* **212** 401
[5] Wolf G H, Wang S, Herbst C A, Durben D J, Oliver W F, Kang Z C and Halvorson K 1992 *High-Pressure Research: Application to Earth and Planetary Sciences* ed Y Syono and H Manghnani (Washington, DC: American Geophysical Union) p 503
[6] Yamanaka T, Shibata T, Kawasaki S and Kume S 1992 *High-Pressure Research: Application to Earth and Planetary Sciences* ed Y Syono and H Manghnani (Washington, DC: American Geophysical Union) p 493
[7] Tsuchiya T, Yamanaka T and Matsui M 1998 *Phys. Chem. Minerals* **25** 94
[8] Tsuchiya T, Yamanaka T and Matsui M 2000 *Phys. Chem. Minerals* **27** 149
[9] Liu L and Mernagh T P 1992 *High Temp.–High Pressures* **24** 13
[10] Vannereau F, Itie J P, Polian A, Calas G, Petiau J, Fontaine A and Tolentino H 1991 *High Pressure Res.* **7** 372
[11] Brazhkin V V, Tatyanin E V, Lyapin A G, Popova S V, Tsiok O B and Balitskii D V 2000 *Pis. Zh. Eksp. Teor. Fiz.* **71** 424
Brazhkin V V, Tatyanin E V, Lyapin A G, Popova S V, Tsiok O B and Balitskii D V 2000 *JETP Lett.* **71** 293 (Engl. Transl.)
[12] Haines J, Leger J M and Chateau C 2000 *Phys. Rev.* B **61** 8701
[13] Prakapenka V B, Dubrovinsky L S, Shen G Y, Rivers M L, Sutton S R, Dmitriev V, Weber H P and Bihan T L 2003 *Phys. Rev.* B **67** 132101
[14] Prakapenka V P, Shen G Y, Dubrovinsky L S, Rivers M L and Sutton S R 2004 *J. Phys. Chem. Solids* **65** 1537
[15] Hemley R J, Jephcoat A P, Mao H K, Ming L C and Manghnani M H 1988 *Nature* **334** 52
[16] Kingma K J, Meade C, Hemley R J, Mao H K and Veblen D R 1993 *Science* **259** 666
[17] Durben D J and Wolf G H 1991 *Phys. Rev.* B **43** 2355
[18] Smith K H, Shero E, Chizmeshya A and Wolf G H 1995 *J. Chem. Phys.* **102** 6851
[19] See, for example, Hadjipanayis G C and Siegel R W (ed) 1994 *Nanophase Materials: Synthesis–Properties–Applications* (Dordrecht: Kluwer–Academic)
Fiorani D and Sberveglieri G (ed) 1994 *Fundamental Properties of Nanostructured Materials* (Singapore: World Scientific)
[20] Jiang J Z 2004 *J. Mater. Sci.* **39** 5103
[21] Wu H P, Liu J F, Ge M Y, Niu L, Wang Y W, Lv G L, Zeng Y W, Wang L N, Zhang G Q and Jiang J Z 2006 *Chem. Mater.* **18** 1817
[22] Mao H K, Bell P M, Shaner J W and Steinberg D J 1978 *J. Appl. Phys.* **49** 3276
[23] Kingma K J, Mao H K and Hemley R J 1996 *High Pressure Res.* **14** 363
[24] Pasternak M P, Rozenberg G Kh, Milner A P, Amanowicz M, Zhou T, Schwarz U, Syassen K, Taylor R D, Hanfland M and Brister K 1997 *Phys. Rev. Lett.* **79** 4409